

# Analysis of Fundus Fluorescein Angiogram Based on the Hessian Matrix of Directional Curvelet Sub-bands and Distance Regularized Level Set Evolution

Asieh Soltanipour<sup>1</sup>, Saeed Sadri<sup>1,2</sup>, Hossein Rabbani<sup>2</sup>, Mohammad Reza Akhlaghi<sup>3</sup>

<sup>1</sup>Departments of Electrical and Computer Engineering, Isfahan University of Technology, <sup>2</sup>Biomedical Engineering, Medical Image and Signal Processing Research Center, Isfahan University of Medical Sciences, <sup>3</sup>Ophthalmology, Isfahan University of Medical Sciences, Isfahan, Iran

Submission: 21-05-2015

Accepted: 08-07-2015

## ABSTRACT

This paper presents a new procedure for automatic extraction of the blood vessels and optic disk (OD) in fundus fluorescein angiogram (FFA). In order to extract blood vessel centerlines, the algorithm of vessel extraction starts with the analysis of directional images resulting from sub-bands of fast discrete curvelet transform (FDCT) in the similar directions and different scales. For this purpose, each directional image is processed by using information of the first order derivative and eigenvalues obtained from the Hessian matrix. The final vessel segmentation is obtained using a simple region growing algorithm iteratively, which merges centerline images with the contents of images resulting from modified top-hat transform followed by bit plane slicing. After extracting blood vessels from FFA image, candidates regions for OD are enhanced by removing blood vessels from the FFA image, using multi-structure elements morphology, and modification of FDCT coefficients. Then, canny edge detector and Hough transform are applied to the reconstructed image to extract the boundary of candidate regions. At the next step, the information of the main arc of the retinal vessels surrounding the OD region is used to extract the actual location of the OD. Finally, the OD boundary is detected by applying distance regularized level set evolution. The proposed method was tested on the FFA images from angiography unit of Isfahan Feiz Hospital, containing 70 FFA images from different diabetic retinopathy stages. The experimental results show the accuracy more than 93% for vessel segmentation and more than 87% for OD boundary extraction.

**Key words:** Diabetic retinopathy, fast discrete curvelet transform, fundus fluorescein angiography, Hessian matrix, level set method

## INTRODUCTION

Diabetic retinopathy (DR) is usually a leading cause of blindness and vision reductions all over the world. A vision screening can be used to detect retinopathy for people who all are at a risk for eye diseases. Detection and localization of main structures in the retinal images, like blood vessels and optic disk (OD) region, have an important role in diagnosis system of DR and some other diseases. Manually extractions of these structures are very time consuming in retinal images and its accuracy (ACC) depends on the user skill level. For this purpose, many methods have been proposed for vessel segmentation and OD localization. A few methods of vessel segmentation and OD detections are explained in the following: Retinal vessel segmentation and description of characteristics of the blood vessels, such as length, width, branching patterns, and angles can be used as an important tools for evaluation of the retinal disorders, macula and OD detection, diagnosis, and screening of various cardiovascular and ophthalmologic diseases, and laser surgery.<sup>[1-3]</sup> According to Fraz,<sup>[1]</sup> vessel segmentation

methods can be done in five main categories: (1) Pattern recognition, (2) matched filtering, (3) vessel tracking/tracing, (4) mathematical morphology, and (5) multi-scale approaches. In each category, several methods are reported in the study by Fraz.<sup>[1]</sup> Pattern recognition techniques can be divided in two categories: (1) supervised methods, and (2) unsupervised methods. An approach based on the back-propagation neural network is described for the segmentation of blood vessels in angiography.<sup>[4]</sup> Two-dimensional (2D) Gabor wavelet and supervised classification is used for retinal vessel segmentation.<sup>[5]</sup> The feature vectors are formed by the pixels intensity and 2D Gabor wavelet coefficients. An algorithm based on feeding a seven-dimensional feature vector composed of gray-level and moment invariant-based features are given to supervised neural network, to extract the vessels.<sup>[6]</sup> The approach can be considered as matched filter method.<sup>[7-9]</sup> A 2D linear kernel with Gaussian profile is introduced for vessel detection.<sup>[7]</sup> Since, a vessel may have any angle, the kernel is rotated in 12 different directions and maximum response in each pixel is retained. Amplitude-modified second order Gaussian filter

### Address for correspondence:

Dr. Hossein Rabbani, Department of Biomedical Engineering, Medical Image and Signal Processing Research Center, Isfahan University of Medical Sciences, Isfahan, Iran. E-mail: h\_rabbani@med.mui.ac.ir

has been proposed for blood vessel segmentation.<sup>[8]</sup> Also, a 2D Gaussian matched filter is used for vessel enhancement, and then a neural network is applied to vessel detection.<sup>[9]</sup> A tracking method with Gaussian and Kalman filters for vessel segmentation in retinal images is proposed.<sup>[10]</sup> The second order matched filter is used for centerline estimation and then tracking process is started. The Kalman filter is applied for the estimation of next vessel location. Also, a modular supervised method for vessel segmentation is proposed.<sup>[11]</sup> The image background is normalized for nonuniform intensity variations using scale space theory and a supervised optimization procedure is applied to determine the optimal scale.

OD region localization is an important landmark feature in retinal image analysis, and its diameter is usually used as a reference for fovea region detection. OD is usually characterized as a brighter component than the rest of ocular fundus from which the blood vessels and optic nerves emerge from it. Recently, many methods are proposed for the OD segmentation. Principle component analysis (PCA) is used to extract OD even for images with bright lesions.<sup>[12]</sup> In this method, a training set using the brightest pixels are produced as OD candidate regions and then, PCA is incorporated to project a new image to disk space. Hough transform method is proposed to locate OD.<sup>[13]</sup> In this method, a circular region is found by first isolating the brightest area in the image using morphological operators and then, a Hough transform is implemented to detect the circular area features within the gradient image resulting from region of interest (ROI). A geometrical directional pattern of the retinal vascular system is used to embed information on the OD location which is the point of convergence of the vessels.<sup>[14]</sup> OD is detected using a vessels direction matched filter from normalized digital fundus images.<sup>[15]</sup> At first, the retinal vessels are detected by a standard 2D Gaussian matched filter. Then, the detected vessels are thinned and filtered using local intensity to represent OD center candidates. OD region is detected by the combination of fast discrete curvelet transform (FDCT) and level set deformable model in color images.<sup>[16]</sup> In this method, OD region candidate is extracted using modified curvelet coefficients and canny edge detector and then, the boundary of OD is extracted by level set deformable model.

This paper presents an automatic system to detect main structures, such as OD and vascular tree, in the fundus fluorescein angiogram (FFA) images. The overview of the proposed method is explained in Section II. The proposed method for vessel segmentation that is a modified version of proposed method which is described in Section III.<sup>[17]</sup> This method contains three main phases: (1) Preprocessing, (2) centerline extraction using information about the first order derivative and eigenvalues obtained from the Hessian matrix of FDCT sub-bands, and (3) tree vessel segmentation using region

growing algorithm. After the segmentation of blood vessels from the FFA images, OD boundary is extracted using a four-phase algorithm. This method is described in Section IV and includes: (1) Removing vessels, (2) candidate OD regions detection using canny edge detector and Hough transform, (3) detecting actual location of OD, using the information of main arc of retinal vessels around the OD region, and (4) extracting OD boundary based on the distance regularized level set evolution (DRLSE) model. After explaining the proposed method in this paper, the experimental results on the FFA images of the Isfahan central eye clinic and the images of DRIVE database are presented in Section V. Finally, Section VI contains the main conclusions of this paper.

## OVERVIEW OF THE PROPOSED METHOD

The functional block diagram of the proposed method in this paper for vessel detection and OD boundary extraction is shown in Figure 1.

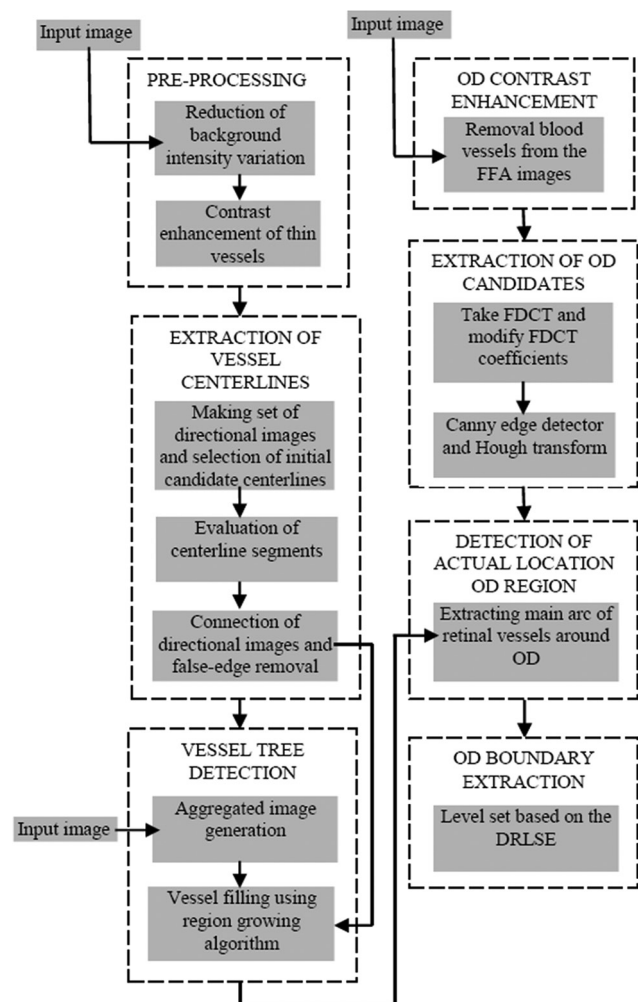


**Figure 1:** Functional block diagram of proposed method. The proposed method for extraction of the blood vessels and of the optic disk location is shown in the left and right columns respectively

The left column of Figure 1 shows the proposed algorithm for segmentation of the blood vessels, where involves three basic processing phases:

1. Preprocessing for reduction of background intensity variation and contrast enhancement of thin vessels.
2. Extraction of vessel centerlines, which this phase involves three sub-steps as follows:
  - First step: Making a set of directional images and extracting initial candidate centerlines based on the information of the first order derivative and the eigenvalues from the Hessian matrix
  - Second step: Evaluation of the centerline segments
  - Third step: Connection of the directional images resulting from two previous steps and removal of the false-edges.
3. Vascular tree segmentation, for complete segmentation of the tree vessels, which combines the vessel centerlines with the set of the images resulting from modified top-hat transform followed by bit plane slicing.

The right column of Figure 1 shows the proposed algorithm for extraction of OD boundary, which includes four main processing phases:

1. Contrast enhancement of the OD region through removing of the blood vessels by using a sequence of dilation and erosion morphological operators.
2. Detecting candidate regions for OD, where this phase includes two sub-steps as follows:
  - First step: Applying FDCT to the image resulting from the contrast enhancement of the OD region phase and modification of the curvelet coefficients.
  - Second step: Applying canny edge detector and Hough transform on the reconstructed image from the modified coefficients curvelet.
3. Detecting convergence point of vessels in order to find the actual location of OD. According to geometrical structure of the blood vessels, main arc of the vessels can be approximated by two lines in directions of  $75^\circ$  and  $105^\circ$  and the intercept point of these two lines can be defined as convergence point of the retinal vessels. The actual location of OD region is obtained using evaluation of the Euclidean distance between the centers of OD candidate regions and the convergence point of the retinal vessels.
4. Extracting OD boundary based on the DRLSE model.

The details of each one of these phases are described in the next sections.

## VESSEL SEGMENTATION

### Image Preprocessing

The image-preprocessing consists of two main phases as follows:

1. Reduction of the background intensity variation: The

background intensity variation of the retinal images makes some of the characteristic of retinal images (e.g., retinal capillaries) to become hardly visible which affects the outcome of the vessel segmentation. Therefore, the background intensity variations are reduced by applying nonlinear diffusion filtering on the original image.<sup>[18]</sup>

2. Contrast enhancement of the thin vessels: To enhance contrast of thin and small vessels, the image resulting from nonlinear diffusion filtering is processed by a sequence of modified top-hat transform iteratively,<sup>[19]</sup> using multi-structure elements morphology. In this paper, the structuring elements with size  $7 \times 7$  pixels are made in 12 different directions with resolution  $15^\circ$ . The detail of the production of structuring elements is available in Eq. (1), which represents the modified top-hat transform:<sup>[19]</sup>

$$\text{Top-Hat}_I = I - \min((I \bullet S) \circ S; I) \quad (1)$$

Where,  $I$  is the output of the nonlinear diffusion filtering to be processed,  $S$  is represented for the multi-structuring elements morphology  $\bullet$  and  $\circ$  are morphological closing and opening operators respectively. Then, the set of the images obtaining from the modified top-hat transform by 12 multi-structuring elements are combined.<sup>[19]</sup> Figure 2 shows the results of this section.

### Vessel Centerlines Extraction

#### Selection of initial candidate centerlines

Since, the retinal blood vessels have a range of different sizes and also can occur in different directions, the analysis of a set of the directional images (and their combinations) in different sizes of the blood vessels' diameter would be informative. So, at first, a set of the directional images based on sub-bands of FDCT is made and then each of these directional images is processed in different sizes blood vessels' diameter for extracting initial candidate centerlines as following:

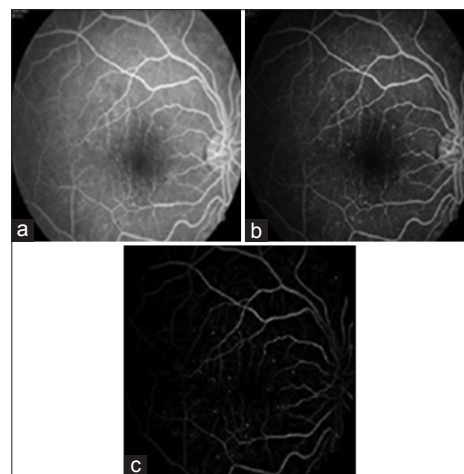


**Figure 2:** (a) Fundus fluorescein angiogram image. (b) Output of nonlinear diffusion filtering. (c) Output of modified top-hat transforms

FDCT is a multi-scale and multi-directional decomposition.<sup>[20]</sup> At first, FDCT is applied on preprocessed image (resulting from Section IIIA). Then, to reconstruct a set of the directional images from the FDCT coefficients, and all coefficients in a specific direction in different scales is preserved, and others are set to zero. In this paper, FDCT via wrapping is applied in 5 scales and 16 directions in the second scales, which makes 32 directions in 3<sup>rd</sup> and 4<sup>th</sup> scales and 64 directions in 5<sup>th</sup> scale. Figure 3 shows a set of the shaded directional wedges in the second to fifth scales which make the first directional image. Under this framework, the number of directional images would be the half number of directional sub-bands in the second scale. So, directional images with frequency contents  $[3\pi/4-(i-1)\pi/8 \quad 3\pi/4+i\pi/8]$  for  $1 \leq i \leq 8$  are obtained, that is, each one of the directional images is averagely directed in the angle defined by:

$$\theta(i) = \frac{(2\hat{\Delta} / 8 - (i-1)\hat{\Delta} / 8) + (2\hat{\Delta} / 8 - i\hat{\Delta} / 8)^0}{2} \quad 1 \leq i \leq 8 \quad (2)$$

According to Gaussian profile of vessels and reduction of intensity values from vessel centerlines to vessel edges in the FFA images, a pixel from the directional images belongs to vessel centerline, if its intensity value is greater than a threshold. So, we would have eight images  $I_i$ , for  $1 \leq i \leq 8$ , which represents the final directional images resulting from this step. Figure 4 shows the directional images  $I_i$ , for  $1 \leq i \leq 8$ .

To process the information of the blood vessels at a specific direction and different scales of the blood vessels' diameter, each one of the directional images  $I_i$  is convolved with a Gaussian kernel  $G(x, y; s(j))$  of variance  $s^2(j)$  according to Eq. (3). Since, the diameter of the blood vessels change logarithmically,  $s(j)$  can be defined by Eq. (4).<sup>[21]</sup>

$$I_{i,s(j)}(x, y; s(j)) = I_i(x, y) \otimes G(x, y; s(j)) \quad (3)$$

$$S(j) = \exp\left(\log(a) + \frac{(j-1)(\log(b) - \log(a))}{(N_s - 1)}\right) \quad (4)$$

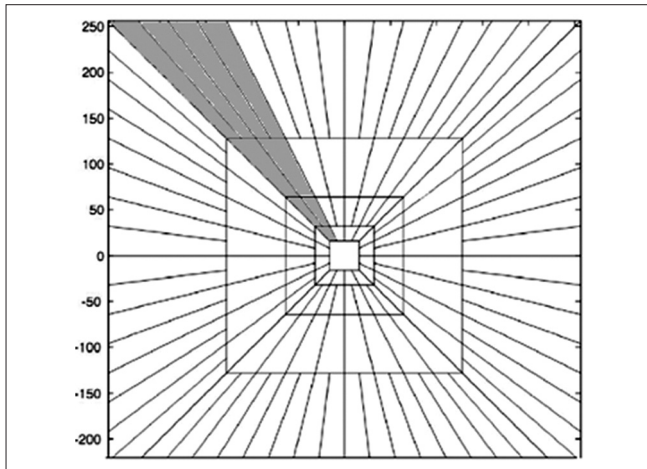


Figure 3: Directional wedges in specific direction in second to fifth scales for making first directional image

In Eq. (3) and (4),  $1 \leq i \leq 8$ ,  $1 \leq j \leq N_s$ ,  $s(j)$  is length of the Gaussian kernel,  $N_s$  is the number of scales and  $a, b$  are minimum and maximum radius of the vessels. In this paper based on the dataset  $a, b$ , and  $N_s$  are considered as 0.4, 2, and 5 respectively. The Gaussian kernel is defined as:

$$G(x, y; s(j)) = \frac{1}{2\pi s(j)^2} e^{-\frac{x^2+y^2}{2s(j)^2}} \quad (5)$$

So,  $I_{i,s(j)}$  in Eq. (3), contains structures with characteristic length  $< s(j)$ , which are directed in angle  $\theta(i)$ .

Also, derivatives of a directional image can be approximated by a linear convolution of the directional image with scale normalized derivatives of the Gaussian kernel as following:

$$\partial^n I_{i,s(j)}(x, y) = I_i(x, y) \otimes s(j)^n \partial^n G(x, y; s(j)) \quad (6)$$

Where,  $n$  is the order of the derivative.

In this paper, to extract initial candidate centerlines, each pixel of the directional images  $I_{i,s(j)}$  is processed using the information of the eigenvalues of Hessian matrix and the first order derivative of  $I_{i,s(j)}$ . On the other hand, to calculate eigenvalues of the Hessian matrix with less sensitivity noise, the vessels in each directional image  $I_i$  must be aligned with the x-axis.<sup>[22]</sup> For this purpose, coordinate axis in each directional image  $I_i$  is rotated with  $\theta(i)$ .<sup>[22]</sup>

Under this framework, the analysis of the first order derivative of  $I_{i,s(j)}$  and the eigenvalues of Hessian matrix is done. The pixel belongs to centerline if the following criteria are satisfied:

### Evaluation of the first order derivative of the directional images

For this purpose, the first order derivative of the directional images  $I_{i,s(j)}$  is calculated along x-axis as:

$$\frac{\partial I_{dir,s(j)}(x, y)}{\partial x} = I_{dir}(x, y) \otimes s(j) \frac{\partial G(x, y; s(j))}{\partial x} \quad (7)$$

Then, each pixel of resulted images from Eq. (7) is investigated for the change of signs of the two its neighboring pixels on perpendicular direction to the direction of the corresponding directional image.

### Eigenvalue analysis

For this purpose, the Hessian matrix for each pixel of directional images  $I_{i,s(j)}$  is defined as:

$$H_{i,s(j)} = S^2(j) \begin{bmatrix} \frac{\partial^2 I_{dir,s(j)}}{\partial x^2} & \frac{\partial^2 I_{dir,s(j)}}{\partial x \partial y} \\ \frac{\partial^2 I_{dir,s(j)}}{\partial x \partial y} & \frac{\partial^2 I_{dir,s(j)}}{\partial y^2} \end{bmatrix} \quad (8)$$

In Eq. (8),  $1 \leq i \leq 8$  and  $1 \leq j \leq 5$ . Also, each one of the elements of the Hessian matrix is calculated by Eq. (6).

Assuming the eigenvalues,  $\lambda_1$  and  $\lambda_2$ , for each pixel of the directional images  $I_{i,s(t)}$ , a pixel from the image belongs to vessel centerline, if the largest eigenvalue from the Hessian matrix is negative. So, each directional image  $I_{i,s(t)}$  is searched for the negative eigenvalue with the maximum magnitude. At the next step, the histogram of the negative eigenvalues with the maximum magnitude is calculated for each directional image  $I_{i,s(t)}$ . The histogram is automatically divided into two parts using Otsu threshold algorithm. Each pixel with the eigenvalue greater than Otsu threshold belongs to an initial centerline point. For those pixels, which are below the Otsu threshold, their means and standard values are calculated and each pixel which is greater than the sum of mean and standard value is assigned to an initial centerline point.<sup>[23]</sup>

### Evaluation of centerline candidate segments

Evaluation of centerline selected segments is done in three steps:

- At first step, for each pixel from directional images resulting from previous section, the intensity and

Euclidean norm of eigenvalues are multiplied together. Then, the maximum value of this feature is calculated for each pixel in a specific direction on all scales of Gaussian kernel. Figure 5 illustrates the directional images resulting from this step

- At second step, the directional images resulting from the first step are combined together according to first column of Table 1. Therefore according to third column of Table 1, there will be just four main directions for the images. Figure 6 shows four directional images obtained from Table 1
- At third step, the intensity feature of each candidate segment in four directional images [Table 1] is calculated using geometric mean between the mean and maximum intensity values of the candidate segment.<sup>[23]</sup> Then, the histogram of all candidate segments' intensities in each directional image is automatically divided into two parts using Otsu threshold algorithm. Then, for those pixels which are below the Otsu threshold, their minimum, maximum and standard deviation are

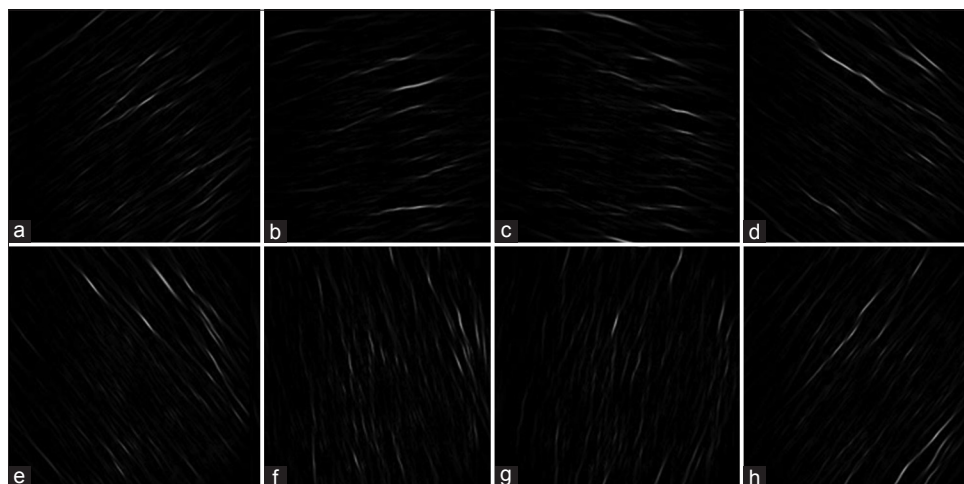


**Figure 4:** (a-h) The figure shows a set of directional images,  $I_i$  for  $1 \leq i \leq 8$ , which is averagely directed in the angles  $33.75^\circ$ ,  $11.25^\circ$ ,  $168.75^\circ$ ,  $146.25^\circ$ ,  $123.75^\circ$ ,  $101.25^\circ$ ,  $78.75^\circ$  and  $56.25^\circ$  respectively

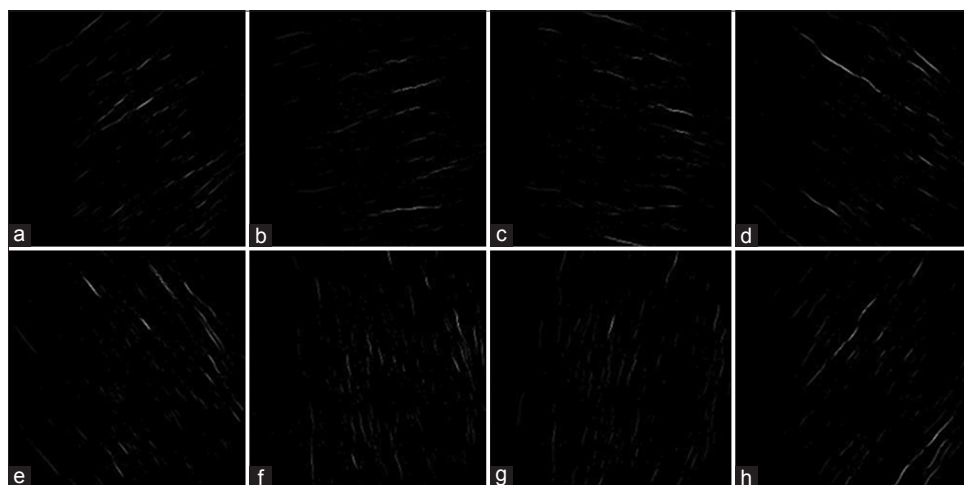


**Figure 5:** (a-h) Set of directional images resulting from evaluation of two features intensity and sum of squares of the eigenvalues on the scales of Gaussian kernel

Table I: Angles of directional images

Directional image of Figure 5	Angle of directional image ( $\Theta_i$ )	Approximated angle
(b)	11.25°	0°
(c)	168.75°	
(a)	33.75°	45°
(h)	56.25°	
(f)	101.25°	90°
(g)	78.75°	
(d)	146.25°	135°
(e)	123.75°	

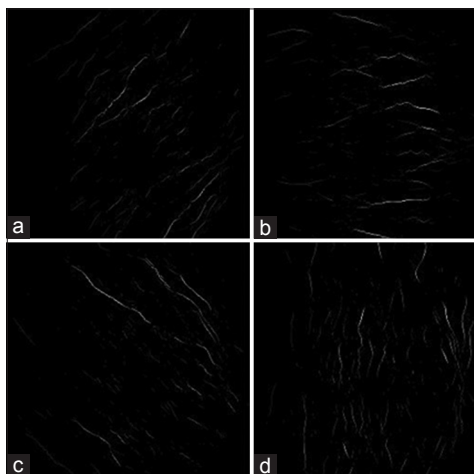


Figure 6: (a-d) Four directional images resulting from Table I (diagonal 45°, horizontal, diagonal 135° and vertical)

calculated and two thresholds  $T_1$  and  $T_2$  are defined as geometric mean between the minimum and standard value and geometric mean between the maximum and standard value, respectively. The candidate segments with intensity value greater than  $T_2$  are considered as vessel centerlines and candidate segments with intensity value smaller than  $T_1$  are removed from the image.

In the next section, the candidate segments with the intensity feature greater than  $T_1$  and smaller than  $T_2$  are processed in order to obtaining the actual centerline segments.

### Connection of directional images and false-edge removal

The directional images resulting from previous section are connected together in two phases:

1. All the centerline segments with the intensity value greater than  $T_2$  of the corresponding directional image are jointed together as shown in Figure 7. The obtained image contains the main and large vessels of the original image
2. The centerline segments with the intensity value greater than  $T_1$  and smaller than  $T_2$  are jointed together as shown in Figure 8. The obtained image contains thin

and small vessels and also a few nonvessel structures of the original image. The nonvessel structures in the resulted image are removed in the following main steps:

Micro-aneurysms (MAs) are the first sign of DR with the similar intensities of the vessels in the FFA images. These nonvessel structures can be observed as more bright spots close to thin and small vessels. To remove these nonvessel structures from the image, at first the candidate segments with length smaller than an experimentally determined threshold are considered. Length of the candidate segment is calculated by maximum number of its pixels in vertical or horizontal direction. Then, maximum and minimum intensities of every candidate segment are considered from the resulted image in Section IIIA. The pixel with maximum intensity is removed from the image, if difference between maximum and minimum intensities is greater than  $T = 50$ . This procedure is repeated until no more pixels are removed.

In this step, each pixel from candidate segments with length value smaller than  $T = 25$  is labeled as a branch, end or curve point by the number of 8-adjanced pixels according to the following rule:

- $n_8 = 1 \rightarrow$  end-point
- $n_8 = 2 \rightarrow$  curve-point
- $n_8 \geq 3 \rightarrow$  branch-point.

Since, MAs can be observed as brighter spots close to thin and small vessels, pixels labeled as branch-point are removed from the image. This is because, they may be the result of MAs.

Finally, two images resulting from this section are jointed together into a binary image and the connected components with the area smaller than  $T = 9$  are removed from the image. Figure 9 shows vessel centerlines image.

### Vascular Tree Detection

Till now we have obtained the centerline of vessels. In order to extract the final vascular tree the following region growing algorithm is applied.

#### Aggregated images generation

In this step, the original image is processed by applying a sequence of the modified top-hat transform by the circular structuring elements according to Eq. (9), where  $S_c$  and  $S_o$  are respectively represented the structuring elements for closing ( $\bullet$ ) and opening ( $\circ$ ) operators.<sup>[22]</sup>

$$top-hat(I) = I - \min(I \bullet S_c) \circ S_o; I \quad (9)$$

In Eq. (9), the morphological close operator, which is a dilation followed by erosion, is applied to generate a smooth version of the original image and erase the variation of background. A circular structuring element of radius 1 pixel

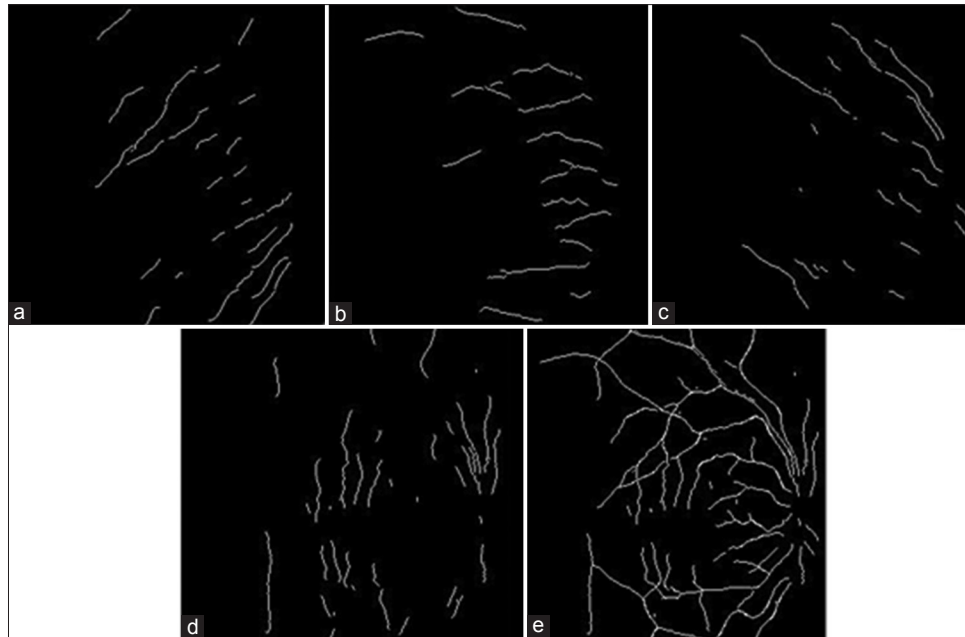


**Figure 7:** (a-d) Centerline segments with the intensity feature greater than threshold  $T_2$  (diagonal  $45^\circ$ , horizontal, diagonal  $135^\circ$  and vertical). (e) Image resulting from connection of candidate segments in (a-d)

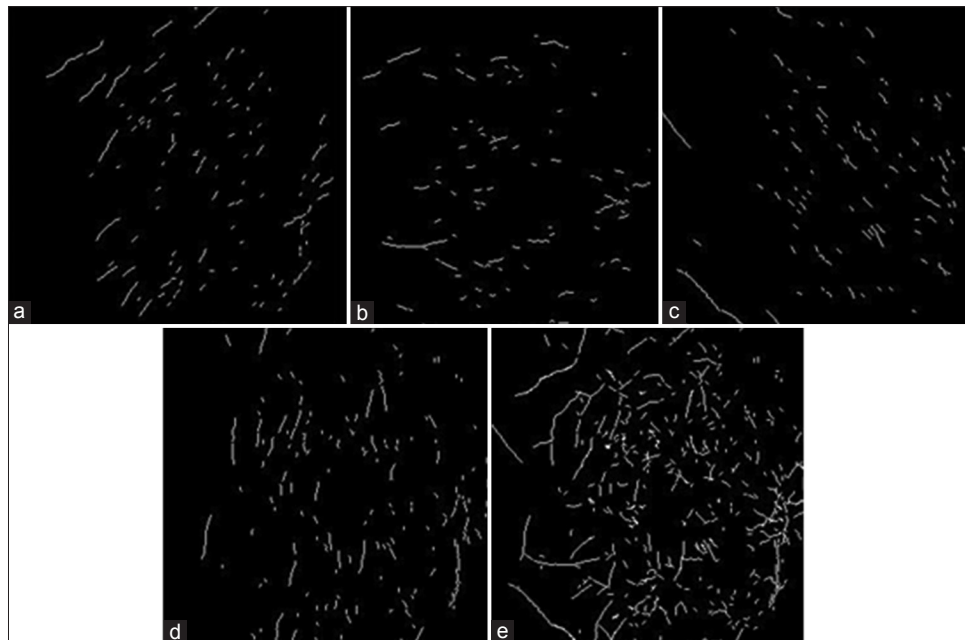


**Figure 8:** (a-d) Centerline segments with the intensity feature greater than threshold  $T_1$  and smaller than  $T_2$  (diagonal  $45^\circ$ , horizontal, diagonal  $135^\circ$  and vertical). (e) Image resulting from connection of directional image in (a-d)

is considered for closing operator. The opening operator, which is an erosion followed by a dilation, is applied to remove those vessels from the image which are smaller in size than the defined structure element. Since retinal blood vessels have a range of different sizes, the circular structuring elements with various radius, 1, 2, 3, and 4 pixels are considered for opening operator. Each of the four final images resulting from modified top-hat transform in Eq. (9) represents the objects of image with size smaller

than the structuring element used for the corresponding opening operator.

Then, to reconstruct potential segments of vessel in each of four directional images resulting from Eq. (9), each one of these images is represented in the form of bit planes, ranging from bit plane 1 to bit plane 8. Bit plane slicing can be used as a useful tool for separating different parts of an image. Table 2 shows bit planes considered for each one of

the four images resulting from Eq. (9). The other bit plans result more details of images and can be appeared as noise in the final image of vascular tree. Finally, the summation of bit plans considered for each one of the resulted images from Eq. (9) is calculated according to Table 2. Figure 10 shows four images resulting from analysis of bit plans slicing. Four images obtained from this section, are considered as aggregated images for region growing algorithm.

### Vessel filling

The final image of the vascular tree is obtained by combining vessel centerlines resulted from Section IIIB with the four images resulting from the analysis of bit plans slicing in previous phase using the simple region growing algorithm as shown in Figure 11.

According to Figure 11, in the first iteration, the vessel centerlines image is used as seed points and the reconstructed image from top-hat transform with the smallest structuring element for opening operator is used as an aggregated image for a simple region growing algorithm. In each of the subsequent three iterations, according to Figure 11, the reconstructed images from top-hat transform with increasing size of structuring element are used as seed points and outputs of the previous region growing steps are used as aggregated image. The final vascular tree segmentation is obtained after implementation of the region growing algorithm in the fourth iteration. Figure 12 shows vessel centerlines and final vessel segmentation using the proposed method.

**Table 2: Bit plans considered for reconstruction images resulting from top-hat transform**

Radius of structuring element $S_o$	Bit plans used
1 pixel	3,4,5,6 and 7
2 pixel	5,6 and 7
3 pixel	5,6 and 7
4 pixel	6,7 and 8

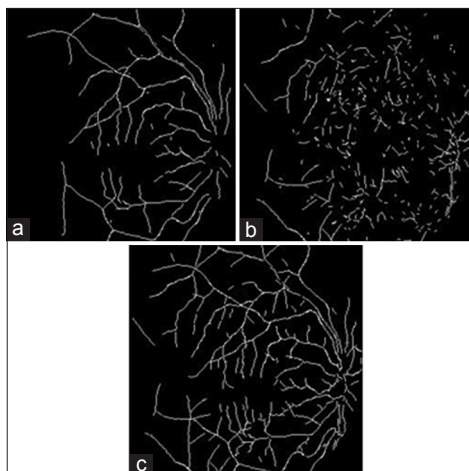


**Figure 9:** (a) Figure 7e. (b) Figure 8e. (c) Detected vessel centerlines

## OPTIC DISK BOUNDARY EXTRACTION

### Optic Disk Contrast Enhancement

OD region extraction can be used as a marker to determine fovea in retinal image and also, has an important role in DR diagnosis. OD in the FFA images is characterized as a bright disk with intensity similar vessels. Given that, the vessels and OD are both bright structures in the FFA images. So, in order to extract OD boundary, at first blood vessels are removed from retinal image. Since, the retinal blood vessels can occur in different directions; to remove blood vessels, the FFA image is processed by a sequence of the dilation and erosion operators, defined by Eq. (10), using the multi-structuring elements. As mentioned in Section IIIA, structuring elements with size  $7 \times 7$  pixels are considered in 12 different directions with resolution  $15^\circ$ . In Eq. (10),  $I$  is the original image,  $S$  is multi-structuring element  $\oplus$  and  $\ominus$  are dilation and erosion operators respectively.

$$F = ((I \oplus S) \ominus S) \quad (10)$$

Each output image from Eq. (10) shows vessels in the same direction of the corresponding structuring element. So, the minimum response in each pixel is calculated for 12 images resulting from Eq. (10) for vessels removal. At next step, to reduce OD fluctuations, the image resulting from vessel removal algorithm is processed by dilation and erosion morphological operators using a disk structuring element with radius of 5 pixels.<sup>[16]</sup> Figure 13 shows the results of this section for OD contrast enhancement.

### Identification of Optic Disk Candidate Regions

In this section, the candidate regions for OD are extracted in two main steps:

Step 1: FDCUT is a multi-directional decomposition approach, which its large coefficients correspond to the bright objects in the image.<sup>[16]</sup> OD in the image resulting from Section IVA

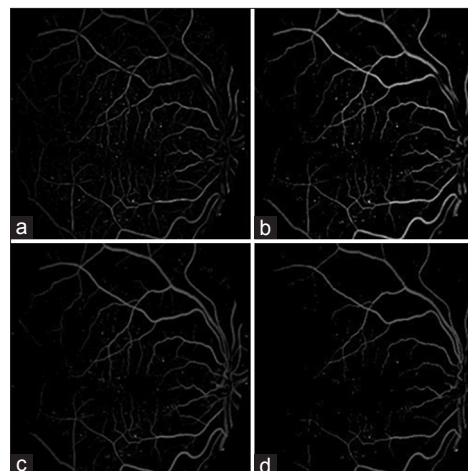


**Figure 10:** (a-d) The images resulting from analysis of bit plans slicing



appears as a bright object, regardless of the background intensity variation. So, OD location can be approximately determined by transforming the enhanced image using FDCT via wrapping and modifying FDCT coefficients by a function  $D_c$  with the exponent of  $P$  which is defined by Eq. (11).<sup>[16]</sup>

$$D_c(x) = x^p \quad (11)$$

In this paper,  $P = 15$  is experimentally selected for modifying FDCT coefficients. Then, the inverse FDCT is applied to modified coefficients to distinguish OD candidate regions from other regions of the image. Figure 14 shows the results of reconstruction of the modified FDCT coefficients for Figure 13.

Step 2: In this step, canny edge detector is applied on the image resulting from the previous step. The background intensity variation around OD region has caused un-circular

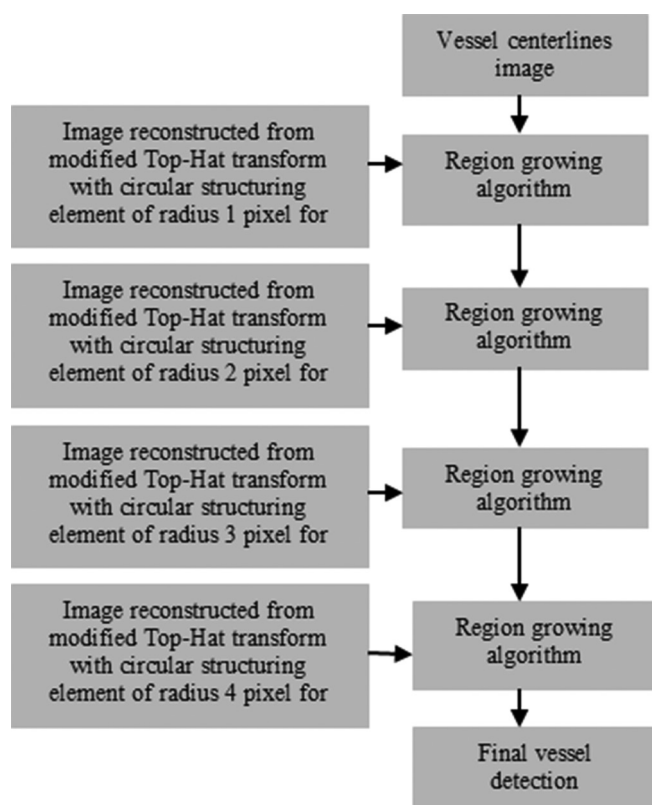


Figure 11: The proposed method for vessel filling

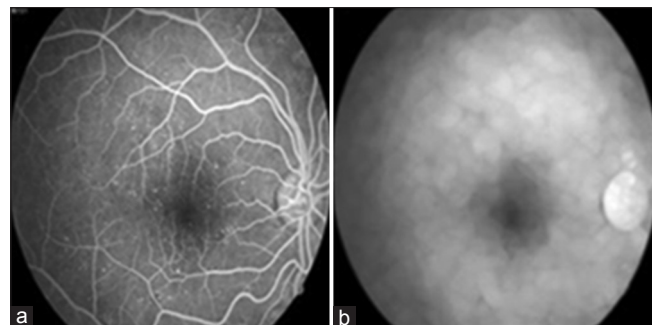


Figure 13: (a) Original image. (b) Optic disk contrast enhancement

structures for OD candidate regions. So, Hough transform is used for reconstructing OD candidate regions resulting from canny edge detector with the un-circular structures in range of radius.<sup>[12]</sup> Figure 15 shows the results of this step.

### Actual Location of Optic Disk Region

Actual location of OD region is determined in three main steps: (1) Extracting the main arc of the retinal vessels around OD region, (2) Determining vertex of the main arc of the vessels in the retinal images (convergence point for retinal blood vessels), (3) Evaluating the Euclidean distance between the centers of OD candidate regions and vertex of the main arc of the retinal vessels.

#### Extracting the main arc of the vessels

The main arc of the retinal vessels around OD region is extracted according to the phases:

Step 1: According to structure of main arc of the retinal vessels around OD region, the image resulting from vessel extraction algorithm, [Figure 12b] is processed by opening operator using the multi-structuring elements with size  $7 \times 7$  pixels which are directed in angles of  $75^\circ$  and  $105^\circ$ . Then, summation of these two images is considered for the next processes. The results of this step are shown in Figure 16.

Step 2: In this step, to determine main arc of the retinal vessels, the length of vessel candidate segments resulting from previous step is calculated by considering the number of pixels in vertical direction. Then, mean and standard value

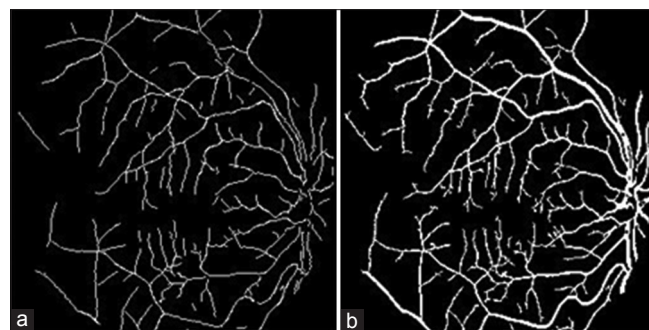


Figure 12: (a) Detected vessel centerlines. (b) Final vessel segmentation

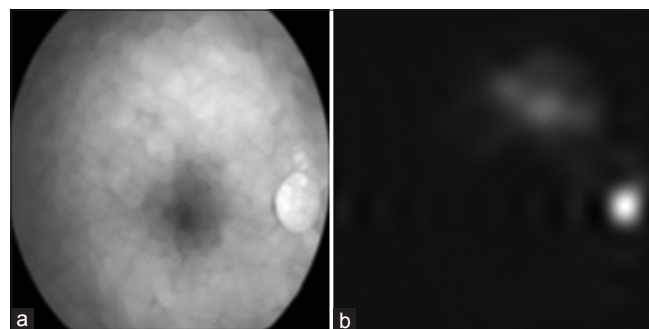
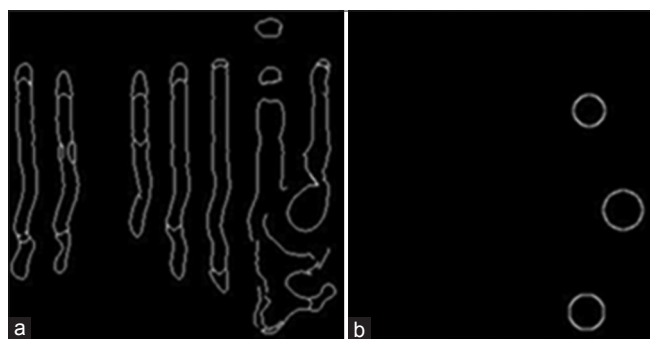


Figure 14: (a) Optic disk contrast enhancement. (b) The image resulting from reconstruction of the modified fast discrete curvelet transform coefficients

of the distribution of length of vessel candidate segments are calculated and the candidate segments with the length smaller than total mean and standard value are removed from the image. Afterward, the center of mass of each segment remaining from previous step is calculated and Euclidean distance between its center of mass and center of mass of other segments is computed. Then, pair of segments with the minimum Euclidean distances is considered and mean of the distribution of Euclidean distances of remained pairs is calculated. Finally, only pair of segments with the Euclidean distances smaller than the mean value is preserved and the others are removed from the image. So, the main arc of the retinal vessels is extracted by implementation of these two steps. Figure 17 shows the main arc of the vessels around the OD region.

### Convergence point of the blood vessels determination

To determine vertex of main arc of the vessels, the image resulting from previous section is processed by applying opening morphological using two linear structuring elements with size  $7 \times 7$  pixels which are directed in angles of  $75^\circ$  and  $105^\circ$ , as shown in Figure 18. Then, each one of the two segments resulting from previous step can be approximated by a line connecting two endpoints of the corresponding segment [violet color in Figure 18]. Finally, intercept point of these two lines can be defined as convergence point of the retinal vessels [marked by red color in Figure 18].



**Figure 15:** (a and b) The images resulting from canny edge detector and Hough transform, respectively

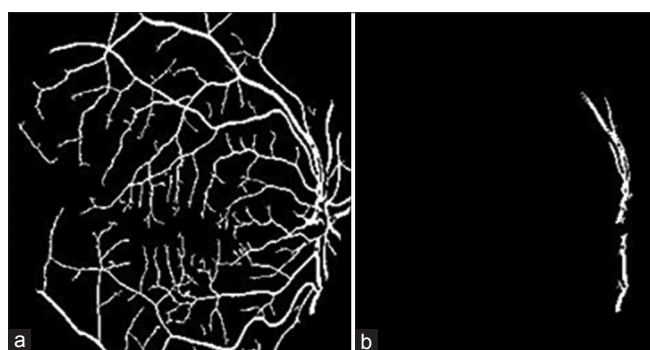


**Figure 17:** (a) Vessels image. (b) Main arc of the vessels around optic disk region

### Evaluation of the optic disk candidate regions

To determine actual location of OD, at first the center of each one of the OD candidate regions, resulting from Section IVB, is considered. Then, the Euclidean distance between the centers of OD candidate regions and the convergence point of the retinal vessels is computed. Finally, the candidate region with the smallest Euclidean distance is considered as the actual location of OD. Figure 19 shows the result of this section.

### OD Boundary Segmentation

In this section, OD region boundary is detected based on the DRLSE model which is defined with a potential function such that the derived level set evolution has a unique forward-and-backward (FAB) diffusion effect.<sup>[24]</sup> The detailed procedure of the DRLSE model is available.<sup>[24]</sup> In this model, initial contour is significantly converged toward the object boundary. For this purpose, the image resulted from

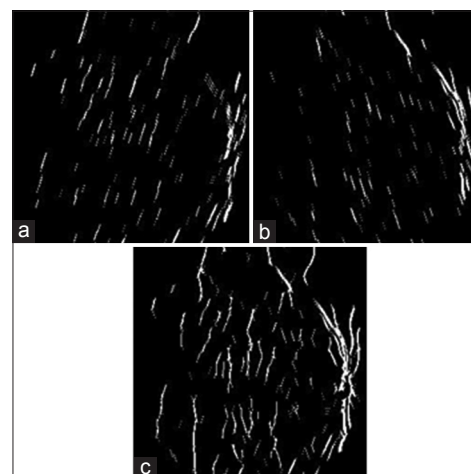


**Figure 16:** (a and b) The images resulting from opening operator by multi-structuring elements with size  $7 \times 7$  pixels in angles of  $75^\circ$  and  $105^\circ$ , respectively. (c) Summation of (a) and (b)

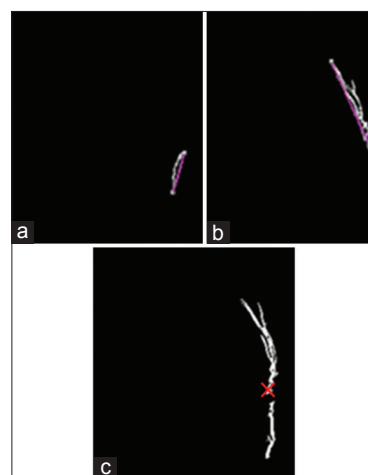


**Figure 18:** (a and b) The images resulting from processing main arc by opening operator using the two linear structuring elements with size  $7 \times 7$  pixels in angle  $75^\circ$  and  $105^\circ$ , respectively. (c) Convergence point of the blood vessels

Section IVC is defined as initial level set contour. The initial level set contour is iteratively converged toward boundary object by the minimization of the total energy function:

$$\frac{\partial \phi}{\partial t} = \mu \operatorname{div}(d_p(\nabla \phi) \nabla \phi) + \lambda \delta_\varepsilon(\phi) \operatorname{div}\left(g \frac{\nabla \phi}{|\nabla \phi|}\right) + \alpha g \delta_\varepsilon(\phi) \quad (12)$$

The first term on the right hand side in Eq. (12) is the level set distance regularization, the second term computes the line integral of the function  $g$  along the zero level set contour of  $\phi$  and this term is minimized while the zero level set contour of  $\phi$  is converged at the boundary object, and the third term is defined for accelerating of displacement of zero level set contour toward boundary object in the level set evolution process.

The parameters used in Eq. (12) are defined as follows:

- $\nabla$  is the Laplacian operator and  $\delta_\varepsilon(x)$  is the smooth version of Dirac delta function with  $\varepsilon = 1.5$  that is defined as:

$$\delta_\varepsilon(x) = \begin{cases} \frac{1}{2\varepsilon} \left[1 + \cos\left(\frac{\lambda x}{\varepsilon}\right)\right], & |x| \leq \varepsilon \\ 0, & |x| > \varepsilon \end{cases} \quad (13)$$

- $g$  is the indicator function and defined by:

$$g = \frac{1}{1 + |\nabla G_\sigma * I|^2} \quad (14)$$

In Eq. (14) image  $I$  is calculated by the summation of the image resulted from Section IVA and the image resulted from the modified FDCT coefficients in Section IVB, in order to get indicator function with more ACC.

- $G_\sigma I$  is the image resulting from the convolution with a Gaussian kernel with standard deviation  $\sigma$ .
- $\lambda > 0$  and  $\alpha \in \mathfrak{R}$  are the coefficients of the energy functional. Note that, if the initial contour is located inside the object, the coefficient  $\alpha$  should be negative and otherwise should be positive.  $\mu > 0$  is defined to control the effect of penalizing the deviation of  $\phi$  from a signed distance function.

Finally, contour  $\phi$  is deformed in each of iteration using equation  $\phi = \phi + \partial \phi / \partial t$  in order to move toward boundary

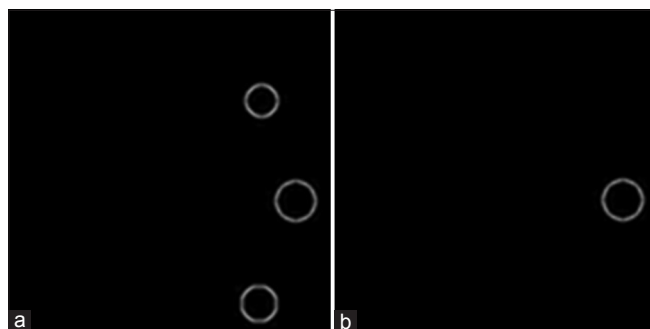


**Figure 19:** (a) Optic disk candidate regions. (b) Actual location of optic disk

of corresponding object. Figure 20 shows the result of this step for  $\alpha = -2$ ,  $\lambda = 10$ ,  $\mu = 0.2$ ,  $\sigma = 1$  after 200 iterations.

## EXPERIMENTAL RESULTS

### Vessel Segmentation Method

Our proposed algorithm for vessel segmentation was tested on the FFA images of size  $576 \times 720$  pixels from angiography unit of Isfahan Feiz Hospital which consist 30 images for normal retinas and 40 images of abnormal retinas. These images can be downloaded from <https://sites.google.com/site/hosseinrabbanikhorasgani/datasets-1/fundus-fluorescein-angiogram-photographs-of-diabetic-patients> or <http://misp.mui.ac.ir/en/Fundus%20Fluorescent%20Angiography%20Images>. Since, our proposed algorithm for vessel segmentation was tested on the FFA images from several patients in different types of diabetic retinopathy in Isfahan Feiz hospital; in order to compare the proposed algorithm with other methods, our vessel extraction algorithm was tested on the green channel of DRIVE database to evaluate the performance of proposed algorithm. The experiments show that the proposed algorithm is more robust for detecting thin and low contrast vessels. The results of the proposed algorithm for vessel segmentation are shown in Figures 21 and 22, for a few samples of the fundus and FFA images of above mentioned databases, respectively. The proposed curvelet-based vessel extraction algorithm according to left column of the functional block diagram in Figure 1 is performed by MATLAB version 8 and the computational time is  $< 2$  min on 4.4 GHz processor CORE i5. In this paper, FDCT via wrapping is applied in 5 scales and 16 directions is defined in the second scales, which makes 32 directions in 3<sup>rd</sup> and 4<sup>th</sup> scales and 64 directions in 5<sup>th</sup> scale to produce directional images.

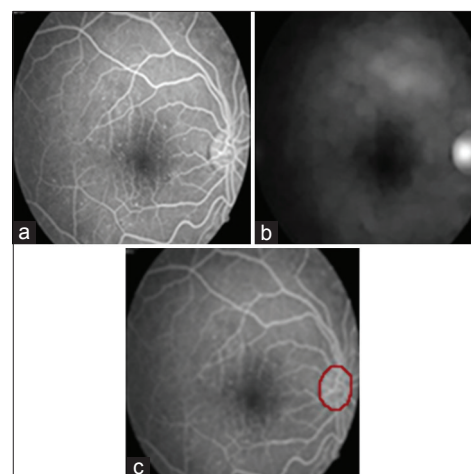


**Figure 20:** (a) Original image. (b) Summation of the image resulting from Section IVA and the image resulting from the modified fast discrete curvelet transform coefficients, in Section IVB. (c) Automated extracted optic disk region

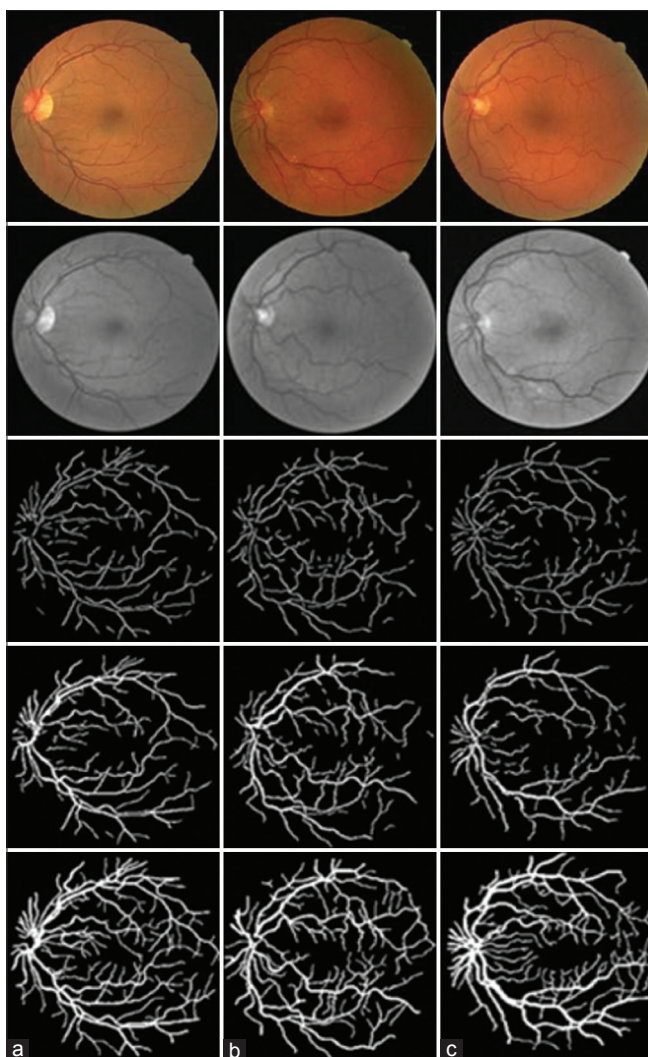


**Figure 21:** (a-c) are related to images 01, 03 and 39 from DRIVE dataset, respectively. From top to bottom, they are the original image, green channel, vessel centerlines, final vessel segmentation and ground truth image, respectively

After obtaining final vascular tree segmentation by iteratively combining vessel centerlines image with the set of images resulting from the aggregated images generation phase, true positive rate (TPR), false positive rate (FPR) and ACC are used to evaluate the results of the proposed algorithm. TPR, FPR and ACC are defined as follows:

$$\text{TPR} = \frac{\text{TP}}{\text{TP} + \text{FN}} \quad (15)$$

$$\text{FPR} = \frac{\text{FP}}{\text{FP} + \text{TN}} \quad (16)$$

$$\text{accuracy} = \frac{(\text{TP} + \text{TN})}{\text{TP} + \text{FP} + \text{TN} + \text{FN}} \quad (17)$$

Where, TP and TN are the blood vessels pixels and background pixels which correctly detected, respectively, FP shows pixels which do not belong to the vessels in the ground truth image but are detected as the blood vessels, and FN shows pixels which belong to vessels in the ground proof image but are

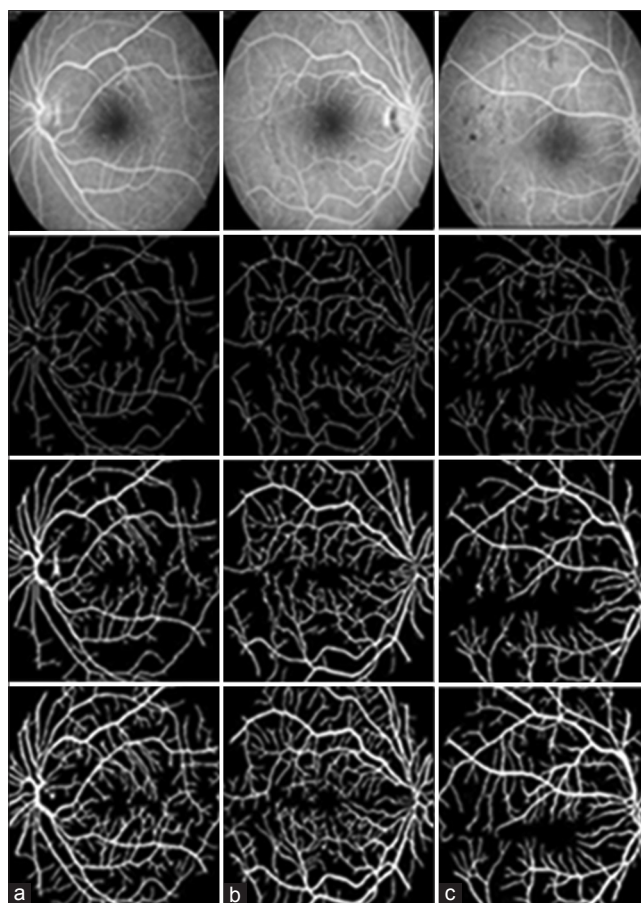


**Figure 22:** (a-c) Related to fundus fluorescein angiogram images from angiography unit of Isfahan Feiz Hospital. From top to bottom, they are the original image, vessel centerlines, final vessel segmentation and ground truth image, respectively

**Table 3:** Comparison of performance between our proposed method for vessel segmentation and others method on DRIVE database

Method	TPR	FPR	Average accuracy
A. M. Mendonca <i>et al.</i> <sup>[23]</sup>	0.7344	0.0236	0.9463
J. Staal <i>et al.</i> <sup>[2]</sup>	0.6780	0.0170	0.9441
M. E. Martinez-Perez <i>et al.</i> <sup>[3]</sup>	0.7246	0.0345	0.9344
D. Marin <i>et al.</i> <sup>[6]</sup>	0.7068	0.0305	0.9452
Our method	0.7068	0.0068	0.9423

TPR – True positive rate; FPR – False positive rate; FFA – Fundus fluorescein angiogram

detected as the background. Table 3 shows the performance of proposed method and other previous approaches in terms of TPR, FPR and ACC for DRIVE database. Also, Table 4 shows the performance of proposed algorithm for vessel segmentation in terms of TPR, FPR and ACC for FFA images from angiography unit of Isfahan Feiz Hospital.

### Optic disk extraction method

Our proposed algorithm for OD extraction has been evaluated on the FFA images of size  $576 \times 720$  pixels from

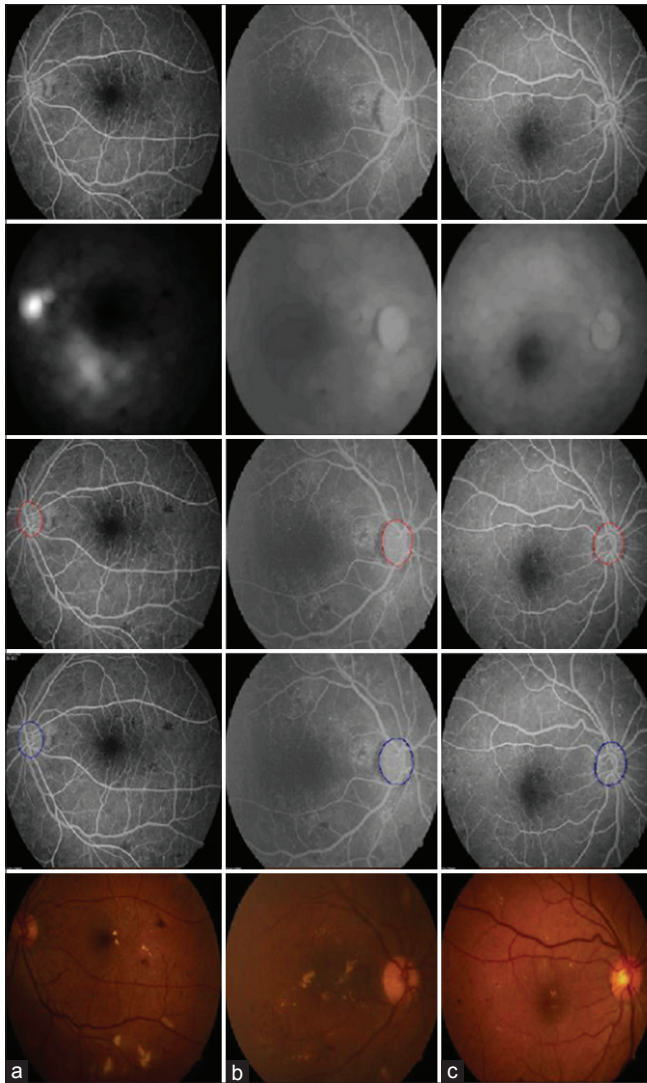


**Figure 23:** (a-c) are related to fundus fluorescein angiogram images of available dataset. From top to bottom, they are input image, image resulting from optic disk contrast enhancement phase, optic disk boundary extraction and manually labeled optic disk region, respectively

available dataset. The proposed method for OD extraction according to right column of the functional block diagram in Figure 1 is applied by MATLAB version 8 and the computational time is less than 1 minutes on 4.4 GHz processor CORE i5. Figure 23 shows the results of the proposed method for a few samples of the FFA images. To evaluate the results of OD extraction, a simple overlap measure is used, that is defined as follows:

$$M = \frac{n(R_a \cap R_g)}{n(R_a \cup R_g)} \quad (18)$$

In Eq. (18),  $R_a$  and  $R_g$  stand for the detected OD region automatically and manually labeled OD region by expert, respectively,  $n(R_a \cap R_g)$  shows the number of pixels in the intersection of  $R_a$  and  $R_g$  and  $n(R_a \cup R_g)$  shows the number of pixels in the union of  $R_a$  and  $R_g$ . Manual detection of the

**Table 4:** The performance measure of vessel segmentation algorithm for FFA images

Method	TPR	FPR	Average accuracy
Our algorithm	0.7362	0.0251	0.9354

TPR – True positive rate; FPR – False positive rate; FFA – Fundus fluorescein angiogram

**Table 5:** The performance measure of OD extraction algorithm for FFA images

Method	TPR	FPR	Overlapping	Overlapping	Overlapping
	$R_a, R_{g1}$ $R_a, R_{g2}$	$R_a, R_{g1}$ $R_a, R_{g2}$	ratio between $R_{g1}, R_{g2}$	ratio between $R_a, R_{g1}$	ratio between $R_a, R_{g2}$
Our algorithm	0.8815 0.8907	0.0002 0.0001	0.8563	0.8005	0.7903

$R_a$  – Detected OD region automatically, and  $R_{g1}$  and  $R_{g2}$  are manually labeled OD regions by first and second experts respectively. TPR – True positive rate; FFA – Fundus fluorescein angiogram; OD – Optic disk

OD is delineated by two experts, independently. Table 5 shows the average performance of proposed method for OD extraction on the defined dataset. In this table, the mean of the overlapping ratio for manually detected OD regions and the mean of the overlapping ratio between OD regions detected automatically and manually are calculated. Also, TPR and FPR of the proposed method are computed using (15) and (16), where TP shows the number of pixels that belonging to OD and are detected by our proposed method correctly, TN shows the number of pixels that do not belonging to OD and our proposed algorithm is not detected them as OD region, FP shows number of pixels that not belonging to OD but our method is detected them as OD region and FN shows number of pixels that belong to OD but our method does not detect them as OD region.

The experimental results show that our proposed method for OD location and boundary extraction are successful in both normal and abnormal images.

## CONCLUSION AND FURTHER WORK

In this paper, a novel algorithm in curvelet domain is introduced for main bright objects in the FFA images. The proposed method starts with the extraction of vessel centerlines. For this purpose, a set of the directional images is made based on the sub-bands curvelet transform. Due to high sensitivity of curvelet transform to the direction in the different scales, curvelet transform is capable of making directional images successfully. Then, each directional image is processed in different sizes blood vessels' diameter based on the information of the first order derivative and the eigenvalues of Hessian matrix for extracting vessel centerlines. The final segmentation of the tree vessel is obtained by combining vessel centerlines with set of images resulting from the top-hat transform followed by bit plane slicing. Since, the retinal blood vessels have a range of different sizes and also can occur in different directions,

the analysis of a set of the directional images in different sizes of blood vessels' diameter (and their combinations) was suitable for extracting thin and small vessels that may be missed in final segmentation. Moreover, there is a trade-off between extracting thin vessels and removing the false-edges and background noise.

Specific characteristics of FFA images make the OD boundary extraction more difficult comparing to color fundus images. Since blood vessels and OD are both bright structures in the FFA images; at first blood vessels are removed from retinal image. Since the bright objects in images are assigned to large curvelet coefficients, FDCT is applied on the image resulting from vessel removal algorithm to determine OD candidate region. Regarding the structure of main arc of the vessel around OD region, actual location of OD is extracted using evaluation the Euclidean distance between the centers of OD candidate regions and convergence point of the retinal vessels. Finally, the boundary OD is extracted based on the DRLSE model, which has a unique FAB diffusion effect. So, the initial contour is iteratively converged toward OD boundary by more ACC. The experimental results show that the proposed method is valid and robust to extract OD boundary in the FFA images.

In this paper we only discussed about the use of curvelet transform for accurate detection of vessels and OD. The segmentation of other important objects in retinal images such as MAs, exudates and fovea region can also be done using the information of vessels and OD. For example, a simple macula detection algorithm can be used by connecting the vessels' end points in a predefined ROI based on OD position. Or MAs and exudates could be extracted after removing bright objects from FFA images and using simple morphological operators.

## ACKNOWLEDGMENTS

The authors would like to thank the angiography unit of Isfahan Feiz Hospital for providing the FFA images of normal and abnormal retinas, also the Image Sciences Institute, University Medical Center Utrecht for making the DRIVE dataset publicly available.

## REFERENCES

1. Fraz MM, Remagnino P, Hoppe A, Uyyanonvara B, Rudnicka AR, Owen CG, et al. Blood vessel segmentation methodologies in retinal images – a survey. *Comput Methods Programs Biomed* 2012;108:407-33.
2. Staal J, Abràmoff MD, Niemeijer M, Viergever MA, van Ginneken B. Ridge-based vessel segmentation in color images of the retina. *IEEE Trans Med Imaging* 2004;23:501-9.
3. Martinez-Perez ME, Hughes AD, Thom SA, Bharath AA, Parker KH. Segmentation of blood vessels from red-free and fluorescein retinal images. *Med Image Anal* 2007;11:47-61.
4. Nekovei R, Sun Y. Back-propagation network and its configuration for blood vessel detection in angiograms. *IEEE Trans Neural Netw* 1995;6:64-72.
5. Soares JV, Leandro JJ, Cesar Júnior RM, Jelinek HF, Cree MJ. Retinal vessel segmentation using the 2-D Gabor wavelet and supervised

- classification. *IEEE Trans Med Imaging* 2006;25:1214-22.
6. Marin D, Aquino A, Gegundez-Arias ME, Bravo JM. A new supervised method for blood vessel segmentation in retinal images by using gray-level and moment invariants-based features. *IEEE Trans Med Imaging* 2011;30:146-58.
7. Chaudhuri S, Chatterjee S, Katz N, Nelson M, Goldbaum M. Detection of blood vessels in retinal images using two-dimensional matched filters. *IEEE Trans Med Imaging* 1989;8:263-9.
8. Gang L, Chutatape O, Krishnan SM. Detection and measurement of retinal vessels in fundus images using amplitude modified second-order Gaussian filter. *IEEE Trans Biomed Eng* 2002;49:168-72.
9. Yao C, Chen HJ. Automated retinal blood vessels segmentation based on simplified PCNN and fast 2D-otsu algorithm. *J Cent South Univ Technol* 2009;16:640-6.
10. Chutatape O, Liu Z, Krishnan SM. Retinal blood vessel detection and tracking by matched Gaussian and Kalman filters. *IEEE Eng Med Biol Soc* 1998;6:3144-9.
11. Anzalone A, Bizzarri F, Parodi M, Storace M. A modular supervised algorithm for vessel segmentation in red-free retinal images. *Comput Biol Med* 2008;38:913-22.
12. Li H, Chutatape O. Automated feature extraction in color retinal images by a model based approach. *IEEE Trans Biomed Eng* 2004;51:246-54.
13. Barrett SF, Naess E, Molvik T. Employing the Hough transform to locate the optic disk. *Biomed Sci Instrum* 2001;37:81-6.
14. Niemeijer M, Abràmoff MD, van Ginneken B. Segmentation of the optic disc, macula and vascular arch in fundus photographs. *IEEE Trans Med Imaging* 2007;26:116-27.
15. Youssif AR, Ghalwash AZ, Ghoneim AR. Optic disc detection from normalized digital fundus images by means of a vessels' direction matched filter. *IEEE Trans Med Imaging* 2008;27:11-8.
16. Esmaeili M, Rabbani H, Dehnavi AM. Automatic optic disk boundary extraction by the use of curvelet transform and deformable variational level set model. *Pattern Recognition*. Vol. 45, July, 2012. p. 2832-42.
17. Soltanipour A, Sadri S, Rabbani H, Akhlaghi M, DoostHosseini A. Vessel Centerlines Extraction from Fundus Fluorescein Angiogram based on Hessian Analysis of Directional Curvelet Sub-bands. In *Proceedings of the 38<sup>th</sup> International Conference on Acoustics, Speech, and Signal Processing (ICASSP)*, Vancouver, Canada; May 26-31, 2013.
18. Li B, Sang N, Cao Z. Contrast-modulated nonlinear diffusion for X-ray angiogram images. *Conf Proc IEEE Eng Med Biol Soc* 2005;2:1736-8.
19. Miri MS, Mahloojifar A. Retinal image analysis using curvelet transform and multistructure elements morphology by reconstruction. *IEEE Trans Biomed Eng* 2011;58:1183-92.
20. Candes E, Demanet L, Donoho D, Ying L. Fast discrete curvelet transforms. *Multiscale Model Simul* 2006;5:861-99.
21. Moghimirad E, Rezatofighi SH, Soltanian-Zadeh H. Multi scale approach for retinal vessel segmentation using medialness function. *IEEE Int Symp Biomed Imaging* 2010;1:29-32.
22. Vakilkandi MJ. "Coronary Vessel Enhancement in Angiograms Using Directional Filter Bank", Ph.D. Dissertation, Department of Electrical Engineering Isfahan University, Isfahan 84156-83111, Iran; 2011.
23. Mendonça AM, Campilho A. Segmentation of retinal blood vessels by combining the detection of centerlines and morphological reconstruction. *IEEE Trans Med Imaging* 2006;25:1200-13.
24. Li C, Xu C, Gui C, Fox MD. Distance regularized level set evolution and its application to image segmentation. *IEEE Trans Image Process* 2010;19:3243-54.

**How to cite this article:** Soltanipour A, Sadri S, Rabbani H, Akhlaghi MR. Analysis of Fundus Fluorescein Angiogram Based on the Hessian Matrix of Directional Curvelet Sub-bands and Distance Regularized Level Set Evolution. *J Med Sign Sence* 2015;5:141-55.

**Source of Support:** Nil, **Conflict of Interest:** None declared

## BIOGRAPHIES



**Asieh Soltanipour** received her Msc in Electrical Engineering from Isfahan University of Technology in 2013. Her main research area are signal, image and video processing.

**E-mail:** asieh.soltanipour@yahoo.com



**Saeed Sadri** is an Associate Professor in Electrical and Computers Engineering Department, Isfahan University of technology, Isfahan, Iran. He received the B.Sc. and the M.Sc. degree in electrical engineering from the University of Tehran,

Faculty of Engineering, Tehran, Iran, respectively in 1977 and 1979. He received the PhD degree in communication engineering from the Isfahan University of Technology, in 1997.

**E-mail:** sadri@cc.iut.ac.ir



**Hossein Rabbani** received the B.Sc. degree in Electrical Engineering (Communications) from Isfahan University of Technology, Isfahan, Iran, in 2000 with the highest honors, and the M.Sc. and Ph.D. degrees in Bioelectrical Engineering

in 2002 and 2008, respectively, from Amirkabir University of Technology (Tehran Polytechnic), Tehran, Iran. In 2007

he was with the Department of Electrical and Computer Engineering, Queen's University, Kingston, ON, Canada, as a Visiting Researcher, in 2011 with the University of Iowa, IA, United States, as a Postdoctoral Research Scholar, and in 2013-2014 with Duke University Eye Center as a Postdoctoral Fellow. He is now an Associate Professor in Biomedical Engineering Department and Medical Image & Signal Processing Research Center, Isfahan University of Medical Sciences, Isfahan, Iran. Dr. Rabbani is a Senior Member of IEEE (Signal Processing Society, Engineering in Medicine and Biology Society, Circuits and Systems Society, Computer Society), and Editor-in-Chief of Journal of Medical Signals and Sensors. His main research interests are medical image analysis and modeling, statistical (multidimensional) signal processing, sparse transforms, and image restoration, which more than 110 papers and book chapters have been published by him as an author or co-author in these areas.

**E-mail:** h\_rabbani@med.mui.ac.ir



**Mohammad Reza Akhlaghi** is an Associate Professor in Department of Ophthalmology, Isfahan University of Medical Sciences, Isfahan, Iran. He received his VitreoRetinal Fellowship in 2006 from the Tehran University of Medical Sciences.

**E-mail:** akhlaghi@med.mui.ac.ir

### "Quick Response Code" link for full text articles

The journal issue has a unique new feature for reaching to the journal's website without typing a single letter. Each article on its first page has a "Quick Response Code". Using any mobile or other hand-held device with camera and GPRS/other internet source, one can reach to the full text of that particular article on the journal's website. Start a QR-code reading software (see list of free applications from <http://tinyurl.com/yzlh2tc>) and point the camera to the QR-code printed in the journal. It will automatically take you to the HTML full text of that article. One can also use a desktop or laptop with web camera for similar functionality. See <http://tinyurl.com/2bw7fn3> or <http://tinyurl.com/3ysr3me> for the free applications.